

SYNTHESIS AND PROPERTIES OF MWCNT-HAP COMPOSITES VIA SOL-GEL TECHNIQUE

J. Jac Faripour Maybody¹, A. Nemati² and E. Salahi^{3*}

* e-salahi@merc.ac.ir

Received: December 2012

Accepted: May 2013

1 Department of Materials Engineering, Science and Research branch, Islamic Azad University, Tehran, Iran.

2 Department of Materials Science and Engineering Sharif University of Technology, Tehran, Iran.

3 Materials and Energy Research Center, Karaj, Iran.

Abstract: In the present study, bioceramic composites based hydroxyapatite (HAp) reinforced with carbon nanotubes (CNTs) was synthesized via sol-gel technique. The dried gels were individually heated at a rate of 5°C/min up to 600°C for 2 h in a muffle furnace in order to obtain HAp-MWCNTs mixed powder. Composites were characterized by XRD, FT-IR, SEM, TEM/SAED/EDX and Raman spectroscopy techniques. Results showed the synthesis of HAp particles in the MWCNTs sol which was prepared in advance, leads to an excellent dispersion of MWCNTs in HAp matrix. Apparent average size of crystallites increased by increasing the percentage of MWCNTs. The average crystallite size of samples (at 600°C), estimated by Scherrer's equation was found to be ~50-60 nm and was confirmed by TEM. MWCNTs kept their cylindrical graphitic structure in composites and pinned and fastened HAp by the formation of hooks and bridges.

Keywords: Ceramic-Matrix composites; Nanostructures; CNT; sol-gel; SEM; TEM.

1. INTRODUCTION

Replacing bone substances has been of particular interest in the development of orthopedic and dental applications, leading to an ever increasing need for the production of artificial hard tissue replacement implants [1]. Research on bioceramics (ceramics, carbon, glass and glass-ceramics) has attracted considerable attention because of their potential for biocompatibility and bioactivity with the human body. Considerable research has been reported in the development of calcium phosphate ceramics as implants. There are many forms of calcium phosphate ceramics that are considered biocompatible [1]. Among the different forms of calcium phosphate, hydroxylapatite (Ca₁₀(PO₄)₆(OH)₂, HAp) is one of the most well-known phases studied for a number of biomedical applications, due to its similar chemical composition and crystal structure to apatite in the human skeletal system [1]. In addition, much research has attempted to enhance the properties of HAp via the addition of secondary ceramic phases for other nonmedical applications. Among different forms of HAp composites, the multi-walled carbon nanotubes (MWCNTs)-HAp composite has drawn

worldwide attention as a candidate for fundamental research studies due to the excellent mechanical properties and chemical stability of CNTs resultant from their cylindrical graphitic structure [1-4]. CNTs, having unique seamless cylinders of graphite sheets either in the form of single-walled (SW) or multi-walled assemblies, exhibit useful properties for various potential applications including miniature biological devices [5]. Also, the electrical properties of CNTs are sensitive to surface charge transfer and changes in the surrounding electrostatic environment, undergoing drastic changes by simple adsorptions of certain molecules or polymers [5-6]. Since the bioactivity of CNTs was reported [7] their use in biomedical application has been anticipated. The most important tissues for preparing CNTs/ceramic composites with high performances are homogenous mixing between CNTs and ceramic powders, retention of perfect structure of CNTs during preparation of composites, strong interfacial bonding between CNTs and matrix, and ensure load translation.

MWCNTs-HAp composites have been prepared using a number of methods such as mechanical mixing, laser surface alloying, chemical vapor deposition, self assembling

technique, plasma-spray, electrophoresis deposition, chemical precipitation, rapid spark plasma sintering method, and biomimetic mineralization [5-9]. However, most synthetic MWCNTs-HAp composites are formed via high temperature processes (e.g. sintering method), resulting in a well-crystallized structure that has little or no activity towards bioresorption [3]. This is in contrast to nanocrystalline or bio-crystal apatites, which are typically non-stoichiometric, and which typically exhibit a much higher degree of bioactivity [4]. Moreover, the sintering of such composites presents difficulties, attributed to the oxidation of CNTs at elevated temperatures [1&8]. Because the MWCNTs-HAp composites fabricated by traditional methods have failed to achieve the desired results, to date the CNTs-reinforced HAp matrix composite has not yet been widely used. In this study formation of MWCNTs-HAp composites using a low temperature sol-gel based method has been studied. This technique, which has to the best of our knowledge not been used to prepare MWCNTs-HAp before, was selected due to the high level of homogeneity that can be obtained using sol-gel based methods. The chemical, physical and mechanical properties of the produced MWCNTs-HAp were investigated to gain information about the phase evolution and microstructure and hence the organization of phases. Very limited information is available in open literature regarding the synthesis of MWCNTs-HAp composites.

Hence, the aim of the present research is to investigate the microstructural characteristics of MWCNTs-HAp powder synthesized via a novel sol-gel method.

2. EXPERIMENTAL PROCEDURE

A multi-wall carbon nanotube (MWCNTs, diameter 10-30 nm, length 15-50 μm , Aldrich, Product ID 636517) was used. The carbon nanotube (CNTs) powder was cleaned in acetone and dehydrated at 473K before mixing with HAp sol. In the sol-gel process, 0.5M phosphorus containing precursor was prepared by addition of P_2O_5 (MERCK Art. No. 540) to ethanol (MERCK Art. No. 1.00971). The resulting ester

was then refluxed at room temperature for 24h. 1.67M solution of $\text{Ca}(\text{NO}_3)_2 \cdot 4\text{H}_2\text{O}$ (MERCK Art. No. 2120) in ethanol was then prepared and mixed for 3h. The phosphorus containing precursor was added drop by drop to the latter solution, while it was stirred vigorously. In a typical synthesis, the above purified CNTs were dispersed into ethanol by sonication for 1h at room temperature to obtain a black homogeneous solution. In the next step, the CNTs sol was added to the HAp sol and stirred for 8h. The gels obtained from the sols were dried at 120 $^\circ\text{C}$ and then heat treated at 600 $^\circ\text{C}$ for 2h to obtain CNTs-HAp composite powder. The crystallinity of the CNTs-HAp samples was characterized by an X-ray diffractometer (XRD, Siemens D-500, Germany) equipped with $\text{CuK}\alpha$ source and operating at 40 KV and 40 mA. The diffraction patterns were obtained at a scan rate of 5 $^\circ\text{min}^{-1}$. Fourier transform infrared (FT-IR, Bruker, Vector 33) spectra were obtained using KBr pellets in the range of 4000-400 cm^{-1} at room temperature. The morphology of selected resulting powder was examined with a Cambridge scanning electron microscope (SEM, XL 30, Philips, Netherland) operating at 25 KV. Finally, transmission electron microscopy (TEM, CM 200 FEG, Philips) was used in characterizing the particles. Raman spectra of the samples were recorded at room temperature and atmospheric pressure on a Renishaw Raman imaging microscope.

3. RESULTS AND DISCUSSION

Fig. 1 shows the XRD pattern of the as-dried state of the gel. All peaks that can be observed in Fig. 1 correspond to calcium nitrate, implying the incomplete reaction between $\text{Ca}(\text{NO}_3)_2 \cdot 4\text{H}_2\text{O}$ and P_2O_5 . No crystalline HAp phase or phosphorus phase could be observed in the XRD pattern, indicating that HAp remains amorphous. Carbon peaks were not significant for their very low weight fraction in the composite. It was observed that crystalline HAp powder appears to form only after performing the heat-treatment at 600 $^\circ\text{C}$ in argon atmosphere [4].

To further study the crystalline structure of the CNTs-HAp nanocomposite, XRD analysis of the

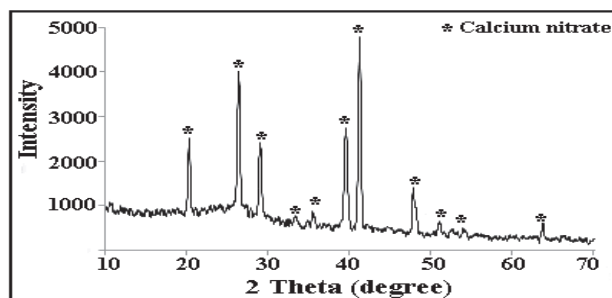


Fig. 1. XRD pattern of the as-dried state of the gel

heat-treatment samples at 600°C were performed. Fig. 2 shows the XRD patterns of HAp-5%CNTs and pure HAp. In these patterns, most diffraction peaks corresponded to those of HAp (JCPD card number 34-0010) [4,9] at 2θ values 21, 23, 26, 29, 30, 31, 34, 40, 48 and 50°, which were indexed to the (200), (111), (002), (210), (034), (211), (202), (310), (213) and (321) planes respectively.

Any peaks corresponding to tricalcium phosphate ($\text{Ca}_3(\text{PO}_4)_2$, TCP) did not appear in Fig. 2. The TCP phase is generally undesired due to the mismatch in degradation rates of HAp and TCP, which may lead to mechanical weakness of the implant [8]. In addition, as shown in Fig.2, no CNTs peaks were found, because the small volume fraction of CNTs introduced into the composites is difficult to detect within the sensitivity limit of XRD. Thus other methods are required to be employed to confirm the existence of residual CNTs in the composites. The broad nature of the diffraction peaks that are seen in

Fig. 2 suggest that the HAp crystals are very small in size. The apparent average crystallite size determined from XRD pattern by Scherrer's equation suggested that broadening is produced by particle size and potential contributions from strain was ignored. The results showed that the apparent average size of crystallites increased by increasing the percentage of CNT (Table 1).

It was also observed that with an increase in aging time, there was a gradual increase in crystal size. It should be noted that the better dispersion of CNTs by the sol-gel method and the resulting higher rate of crystallization can be considered the reason for the larger crystallized fraction. FTIR spectra of raw MWCNT, HAp powder, HAp-1%CNT, HAp-3%CNT and HAp-5%CNT are presented in Fig. 3. Clearly, the IR spectrum for the gels calcined at and above 600°C shows two bands from 600 to 500 cm^{-1} and from 1000 to 900 cm^{-1} , which can be attributed to the absorption modes associated with the presence of PO_4 groups. These bands gradually become

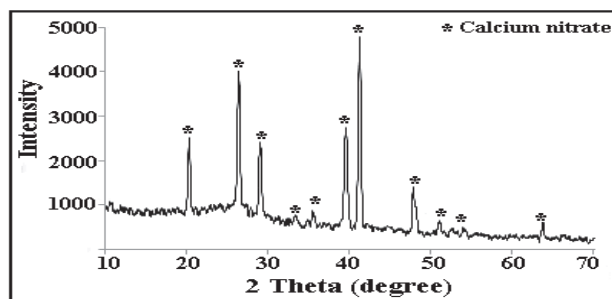


Fig. 2. XRD patterns of samples (a) HAp-5% CNTs and (b) pure HAp

Table 1. The apparent average size of crystallites determined by Scherrer’s equation

Sample	Crystal Size (nm)	
HAP	30.0	
HAP-1%CNTs	52.7	
HAP-3%CNTs	70.0	
HAP-5%CNTs	74.3	

sharper as the CNTs increase. The obvious peaks pertaining to the HAp phase are hydroxyl bands at 3570 cm^{-1} and the symmetrical stretching phosphate ν_1 at around 960 cm^{-1} [4]. It is considered that the peaks at 3450 and 630 cm^{-1} (a small shoulder) correspond to (OH^-) stretching mode. They are the characteristic peaks for stoichiometric HAp, confirming the XRD results for pure stoichiometric HAp. The spectrum also showed the stretching modes of carbonate ions and hydroxyl groups which implied the formation of CNTs on the HAp matrix. The absorption bands observed in the range of $1300\text{--}1650\text{ cm}^{-1}$ are due to the stretching and bending modes of C-O and P-O bands and air carbonate $(\text{CO}_3)^{2-}$ ions, which appear sharper when the CNTs increase (because of the high surface area of the CNTs). The presence of the carbonate peaks in this study could be due to contamination from the air. The distinct shoulder at 868 cm^{-1} (with an increase in CNTs) indicates the presence of HPO_4^{2-} in the structures, and the bands around 2923 cm^{-1} and 2854 cm^{-1} are due to the

asymmetric and symmetric stretching of C-H band.

Fig. 4 shows SEM images of raw MWCNTs with smooth surface and open-ended CNTs (outside diameters of $10\text{--}30\text{ nm}$, inside diameters of $3\text{--}10\text{ nm}$), and a micrograph of HAp-5%CNTs dried gel powder (dried at 120°C for 8 h). The agglomerated hydroxyapatite was caused primarily by the various processes occurring during the drying of gel precursor, and it is also possible that the small particles seen embedded in each agglomerated cluster correspond to calcium nitrate particles possibly obtained from the recrystallization of dissolved calcium nitrate during gel formation and the subsequent drying process. It is known that MWCNTs tend to aggregate because of Van Der Waals forces between nanotubes. Experiments showed that the powders synthesized with a long aging time were larger than those synthesized with a short aging time, showing that aging could contribute to powder growth and agglomerate.

Fig. 5 shows micrographs (at different

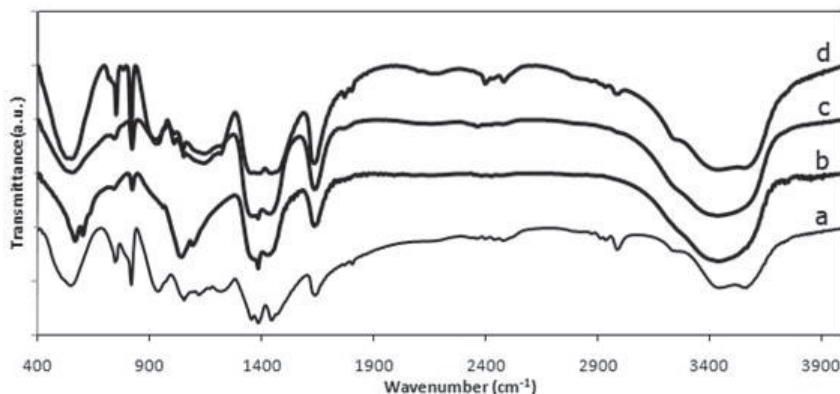


Fig. 3. FT-IR spectra of (a) HAp powder, (b) HAp-1%CNT, (c) HAp-3%CNT and (d) HAp-5%CNT

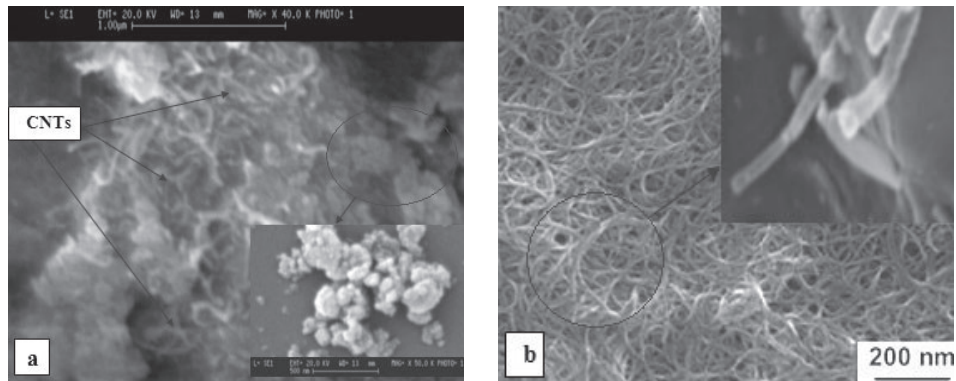


Fig. 4. Typical SEM images of (a) HAp-5%vol CNTs and dried gel powder (120°C for 8h) (b) raw MWCNTs

magnification) of powders that were obtained after heat-treatment at 600 °C. The arrows highlight CNTs in each micrograph. It can be seen that the CNTs are evenly distributed throughout the sample with no diffusion zone around the tubes. Fig 5b shows a unique multilayered morphology, resembling that of natural rock formed by biomineralization. It was clearly seen that CNTs still kept their cylindrical graphitic structure. Production of this kind of multilayered plate-like morphology can contribute to the growth of HAp crystals between the bundles of MWCNTs. It is well known that the CNTs are extraordinarily flexible under large strains and resist failure under repeated bending. This implies that the introduced CNTs in the HAp composite should allow fracture energy absorption or dissipation under stress, and

significantly improves the fracture toughness of HAp composite. Observation from TEM micrographs confirmed that HAp particles showed similar morphological rod-like and spherical structures. The results of the TEM investigation also indicate that the morphology of the powders is strongly related to the Ca/P molar ratio of the solutions. It proves that CNTs have been successfully introduced into HAp matrix and, in addition, that the CNTs might still possess their excellent mechanical properties.

Fig. 6 shows an image of HAp powder, which confirms the presence of multi-walled CNTs with good hollowness and high purity. The amount of attachment appears small, whereas an agglomerated structure appears over a large area. It is believed that sonication during the sample preparation for TEM agglomerates the HAp

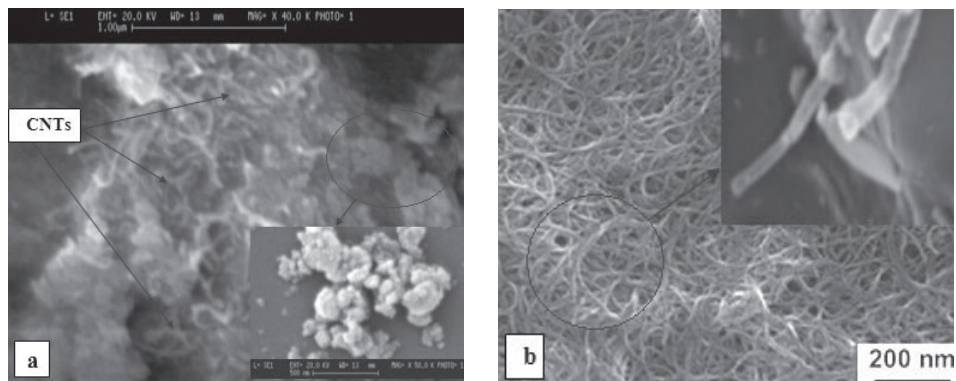


Fig. 5. SEM micrographs of synthesized HAp-CNTs powders at different magnifications

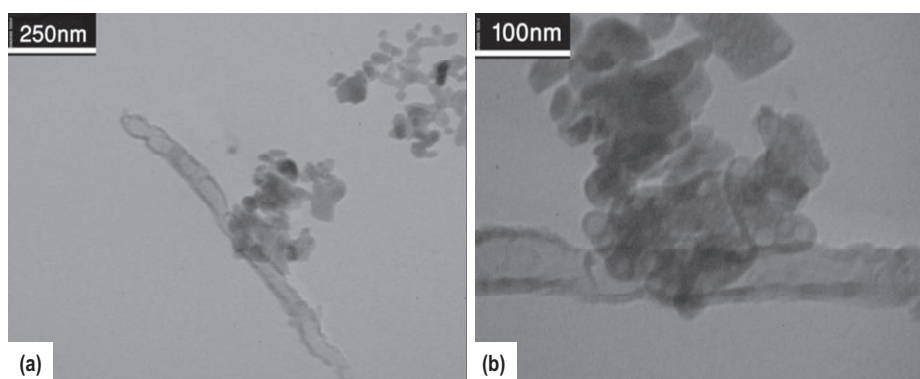


Fig. 6. TEM images of MWCNTs-HAp crystal taken at different magnifications

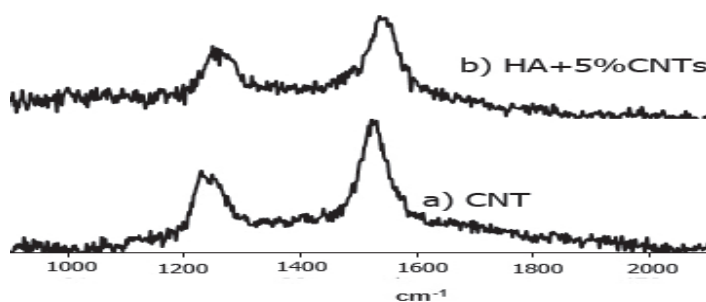


Fig. 7. Raman spectrum of the as-obtained composite powders of CNTs ($I_D/I_G=0.62$) and HAp+5%CNTs ($I_D/I_G=0.75$)

crystals over CNTs. Interaction with HAP powder results in further granulated surfaces, indicating particle attachment on the CNTs surface. It can be seen that the length of CNTs is of the order of several microns. The hydroxyapatite nanoparticles are almost spherical and irregularly hexagonal, with widths and lengths in the range 30-150 nm.

The as-obtained composite powder was also characterized by Raman spectroscopy in detail to validate the presence of CNTs. The typical Raman spectroscopy (Fig. 7) performed on the composite powders distinctly exhibits two peaks ($1280-1350\text{ cm}^{-1}$ and 1572.7 cm^{-1}) for multi-walled CNTs with $I_D/I_G=0.62$. These peaks are associated with the vibrations of carbon atoms with dangling bonds for the in plane terminations of disordered graphite and the vibrations in all sp^2 bonded carbon atoms in a 2-dimensional hexagonal lattice, respectively. The intensity ratio

of D to G band (I_D/I_G) was calculated to be 0.75 for HAP-5%CNTs. The low relative intensity of D to G band implies that the obtained CNTs are mainly composed of well-crystallized graphite, in agreement with the SEM and TEM observations.

CONCLUSIONS

1. No crystalline HAP phase or phosphorus phase could be observed in the XRD pattern due to incomplete reaction between $\text{Ca}(\text{NO}_3)_2 \cdot 4\text{H}_2\text{O}$ and P_2O_5 as starting materials and indicating that synthesise HAp was remained amorphous.
2. Crystalline HAP powder was appeared to form only after performing the heat-treatment at 600°C in argon atmosphere. Any peaks corresponding to tricalcium phosphate ($\text{Ca}_3(\text{PO}_4)_2$, TCP) was not appeared.

3. The average crystallite sizes of composites were determined from XRD pattern by Scherrer's equation and showed that the average sizes of crystallites increased by increasing the percentage of CNTs and by increasing in aging time, a gradual increase in crystal size was observed.
 4. The introduced CNTs in the HAp composite, should allow fracture energy absorption or dissipation under stress, and significantly improves the fracture toughness of HAp composite.
 5. Observation from TEM micrographs confirmed that HAp particles showed similar morphological rod-like and spherical structures. Also showed that CNTs have been successfully introduced into HAp matrix.
- nanotubes in liquids", *J. Des. Sci.* 24 (2003) 1-41.

REFERENCES

1. Li, Y., Hulbert, K., "An Introduction to Bioceramics", *J. Mater. Lett.* 15 (1971), pp. 123-130.
2. Chen, Y., Zhang, Q., "Physical properties of carbon nanotubes", *J. Carbon.* 44 (2006), pp. 37-42.
3. Shen, O., Chen, S. M., Zeng, Q., "Novel Synthesis of lace-like nanorods carbon nanotubes by hydrothermal Conversion Method", *J. Mater. Lett.* 61 (2007), pp. 4280-4282.
4. Shiny, V., Ramesh, R., Sunny, M. C., Varma, H. K., "Synthesis of Inorganic and organic composite", *J. Mater. Lett.* 46 (2000), pp. 35-39.
5. Denissen, H. W., Kalk, V., Nieuport, H. M., Mangano, C., "Handbook of Biomaterials Properties", *J. Inter. Prosth.* 20 (1991), pp. 4-9.
6. Yang, Y., Grulke, E. A., Yang, Z. G., "Rheological behavior of carbon nanotube and graphite nanoparticle dispersions", *J. Carbon.* 5 (2005), pp. 571-579.
7. Jiang, L., Gao, L., "Production of aqueous colloidal dispersions of carbon nanotubes", *J. Collo. Inter. Sci.* Vol. 260 (2000), pp.89-94.
8. Bandyopdhyaya, R., Nativ-Roth, E., Regev, O., Yerushalmi-Rozen, R., "Stabilization of individual carbon nanotubes in aqueous solutions", *J. Mater. Lett.* 2 (2002). pp. 25-28.
9. Hild, J., Grulke, E., "Dispersion of carbon